

## 1 **Pleistocene climate change and the formation of regional species pools**

2 Calatayud, J.<sup>1,2</sup>, Rodríguez, M. Á.<sup>1</sup>, Molina-Vengas, R.<sup>3</sup>, Leo, M.<sup>4</sup>, and Hortal, J.<sup>2</sup>.

3

4 1 Departamento de Ciencias de la Vida, Universidad de Alcalá, Edificio de Ciencias, Ctra. Madrid-  
5 Barcelona km. 33,6, 28871 Alcalá de Henares, Madrid, Spain.

6 2 Departamento de Biogeografía y Cambio Global, Museo Nacional de Ciencias Naturales  
7 (MNCN-CSIC), C/José Gutiérrez Abascal 2, 28006 Madrid, Spain.

8 3. Institute of Plant Sciences, University of Bern, Altenbergrain 21, Bern 3013, Switzerland

9 4. Departamento de Biodiversidad y Conservación. Real Jardín Botánico de Madrid (CSIC).  
10 28014 Madrid, España

11

### 12 **Abstract**

13 Despite the description of bioregions dates back from the origin of biogeography, the  
14 processes originating their associated species pools have been seldom studied. Ancient  
15 historical events are thought to play a fundamental role in configuring bioregions, but  
16 the effects of more recent events on these regional biotas are largely unknown. We  
17 use a network approach to identify regional and sub-regional faunas of European  
18 *Carabus* beetles, and analyse the effects of dispersal barriers, niche similarities and  
19 phylogenetic history on their configuration. We identify a transition zone matching the  
20 limit of the ice sheets at Last Glacial Maximum. While southern species pools are  
21 mostly separated by dispersal barriers, in the north species are mainly sorted by their  
22 environmental niches. Strikingly, most phylogenetic structuration of *Carabus* faunas  
23 occurred since the beginning of the Pleistocene. Our results show how extreme recent  
24 historical events –such as Pleistocene climate cooling, rather than just deep-time  
25 evolutionary processes, can profoundly modify the composition and structure of  
26 geographic species pools.

27

### 28 **Introduction**

29 Naturalists have long been captivated by the geographic distribution of world biotas.  
30 Rooted in the seminal ideas by Alexandre von Humbolt, this fascination has promoted  
31 a long-term research agenda aiming to delineate biogeographic regions according to

32 their integrating faunas and floras (e.g. Wallace 1876, Holt et al. 2013, Rueda et al.  
33 2013). Regional biotas are known to determine ecological and evolutionary dynamics  
34 taking place at finer scales (Ricklefs 2008, 2015). For instance, regional species pools  
35 can modulate local diversity patterns (Ricklefs 2011, Medina et al. 2014, Ricklefs and  
36 He 2016), the structure and functioning of ecosystems (Naeslund and Norberg 2006),  
37 or co-evolutionary processes (Calatayud et al. 2016a). However, despite their  
38 fundamental importance, the processes that have configured regional biotas have  
39 been seldom studied (and particularly the historical ones), and most explanations on  
40 their origin and dynamics remain largely narrative (Crisp et al. 2011).

41 Perhaps the earliest speculations about the formation of regional species pools took  
42 place during the flourishing of bioregionalizations in the mid-19th century (reviewed  
43 by Ebach 2015). During that time, and beyond referring to physical factors (climate,  
44 soils, and physical barriers), some authors already started to emphasize historical  
45 influences as key elements determining the configuration of plant and animal regions.  
46 For instance, when Wallace (1876) proposed his famous zoogeographic regions, he  
47 argued that while the distribution of ancient lineages such as genera and families would  
48 more likely reflect major geological and climatic changes spanning the early and mid-  
49 Cenozoic, that of species would be more influenced by recent events such as  
50 Pleistocene glaciations (see Rueda et al. 2013). Indeed, these recent events could have  
51 fostered many additions and subtractions of species to regional faunas through  
52 dispersal and diversification processes. Increasing evidence suggests that Pleistocene  
53 glacial-interglacial dynamics may have driven population extinction (e.g. Barnes et al.  
54 2002), allopatric speciation in glacial refugia (e.g. Johnson et al. 2004) and post-glacial  
55 recolonization events (e.g. Hewitt 1999; Theissinger et al. 2013). As a consequence,  
56 Pleistocene glaciations are known to influence current diversity patterns for many  
57 taxa, particularly in the Holarctic (e.g. Svenning and Skov 2007; Hortal et al. 2011;  
58 Calatayud et al. 2016b). However, the role of Pleistocene glaciations in shaping  
59 regional species pools remains largely unknown.

60

61 Besides historical contingencies, niche-based processes may also determine the  
62 composition of regional species pools (Mittelbach and Schemske 2015), mainly  
63 throughout their effects on species distribution ranges (Soberon 2007, Hortal et al.

64 2010, Hortal et al. 2012). These processes integrate responses to abiotic conditions  
65 along geographical gradients and to local and regional biotic environment (Colwell et  
66 al. 2009). Furthermore, they involve a complex interplay between evolutionary,  
67 ecological and biogeographical factors. For instance, species with similar climatic  
68 tolerances can coexist in regions of similar climate, but their arrival (and *in situ*  
69 evolution) may be constrained by geographical barriers, which may also lead to  
70 climatic-tolerance divergent species pools (Fig.1a). Further, if species' resemblance in  
71 climatic tolerance is phylogenetically constrained, climate-driven regional species  
72 pools will be also composed of evolutionary related species (i.e. phylogenetically  
73 clustered species pools), although this effect is again filtered by biogeographical  
74 processes (Gouveia et al. 2014). Indeed, diversification of lineages within regions  
75 separated by strong dispersal barriers (e.g. mountain ranges) may also lead to  
76 phylogenetically clustered species pools (Warren et al. 2014; Fig.1a). Over the mid-  
77 term, historical contingencies may contribute to erase the signature of such  
78 geographically-linked diversification. For example, differential diversification rates may  
79 be the predominant driver of regional species pools in climatically stable regions  
80 (Cardillo 2011), yet regions where Pleistocene glaciations exerted a greater influence  
81 may harbour pools of species shaped by the joint effects of current climate and post-  
82 glacial dispersion (Svenning et al. 2015).

83

84 In this study we aim to disentangle the relative importance of the processes that may  
85 contribute to the formation of regional species pools, using European *Carabus*  
86 (Coleoptera: Carabidae) as a model lineage. *Carabus* is a species-rich ground beetle  
87 genus of great popularity due to the beautiful jewel-like appearance of some species  
88 (Turin et al. 2003). In general, *Carabus* species are flightless nocturnal predators of  
89 snails, earthworms and caterpillars. They hold hydrophilic adaptations and are typically  
90 associated to deciduous forests (Deuve et al. 2012). Previous evidence suggests that  
91 the richness of species from this genus in Europe is determined to a large extent by  
92 both current environmental conditions (i.e. climate and habitat) and glacial-interglacial  
93 dynamics (Calatayud et al. 2016b). This makes European *Carabus* an ideal case study to  
94 evaluate the joint effects of evolutionary, ecological and historical contingency  
95 processes as drivers of regional species pools.

96  
97 Specifically, we use data on the distribution and evolutionary relationships of *Carabus*  
98 species, and network and phylogenetic analyses, to evaluate six hypotheses: First,  
99 given the presumed low dispersal capacity of the species from this genus, we  
100 hypothesize that (H1) European *Carabus* species pools are mainly shaped by the main  
101 orographic barriers of the continent, but also, that (H2) glacial-interglacial dynamics  
102 have led to strong differentiation between northern and southern regional species  
103 pools. If this differentiation is true, (H3) northern European *Carabus* faunas will be  
104 composed of species adapted to cold climatic conditions that colonized newly vacant  
105 habitats after the withdrawal of the ice sheet, and hence their regional distribution will  
106 be mostly determined by current climate. In contrast, (H4) southern faunas will be  
107 mainly shaped by the joint influence of diversification events and dispersal limitations,  
108 due to the combined effect of higher climatic stability towards southern latitudes (e.g.  
109 climatic refugia) and a more complex orography (Alps, Pyrenees, Carpathians).  
110 Therefore, (H5) species forming northern regional pools will exhibit comparatively  
111 lower levels of regional endemism, whereas those forming southern regional pools  
112 will show comparatively higher levels of regional fidelity. Finally, according to Wallace  
113 (1876), the advance and retreat of the ice sheets during the Pleistocene should have  
114 determined the spatial distribution of lineages, eroding the effects of the former  
115 configuration of the distribution of the main *Carabus* lineages. Therefore, (H6) we  
116 expect a temporal signal coincident with the Pleistocene in the phylogenetic structure  
117 of *Carabus* faunas, and no effect of deep-time events on the current geographical  
118 distribution these lineages.

119

120

## 121 **Material and methods**

122

### 123 **Data origin**

124 Data on the European distribution of *Carabus* species comes from a recent analysis on  
125 the determinants of diversity of this genus in the continent (Calatayud et al. 2016b).  
126 Briefly, expert-based range maps of all *Carabus* species inhabiting Europe (n = 131)  
127 delineated by Turing et al. (2003) were digitized and overlaid into a 100-km equal-area

128 grid using ARCGIS (grid available at <http://dataservice.eea.europa.eu>). The resulting  
129 gridded distribution maps were reviewed by several experts, eventually correcting cells  
130 wrongly classified as either presences or absences (see Calatayud et al. 2016b for  
131 further details). The resulting presence-absence matrix was used to represent the  
132 distribution of *Carabus* species in all analyses.

133

134 We used environmental and physical geography GIS data from several commonly used  
135 public domain digital repositories. Bioclimatic variables were extracted from Worldclim  
136 (v1.4 Hijmans et al. 2005; available at <http://www.worldclim.org/>). Altitudinal data  
137 were derived from the 30-arcsecond digital elevation model GTOPO30 provided by the  
138 U. S. Geological Survey (available at <https://lta.cr.usgs.gov/GTOPO30>), and the location  
139 of water bodies was extracted from vector information coming from Natural Earth  
140 (available at <http://www.naturalearthdata.com/>). Finally, data for the geographical  
141 distribution of forest habitats come from MODIS Land Cover (Channan et al. 2014,  
142 available at <http://glcf.umd.edu/data/lc/>).

143

## 144 **Statistical analyses**

### 145 **Rationale and structure of the analyses**

146 Exploring the determinants of regional faunas requires analysing ecological,  
147 evolutionary and historical factors jointly. We did so through three consecutive steps  
148 (Fig.1b). First, we identified distinct regional species pools within Europe by using a  
149 network community detection algorithm. From this analysis we derive a species  
150 pairwise similarity matrix of occurrence into different modules that represent different  
151 regions. Second, we assessed the relative importance of the environmental, spatial  
152 and evolutionary determinants of such similarity. We constructed four pairwise  
153 matrices to describe the relationships among species; namely, *i*) a matrix of climatic  
154 niche similarity, *ii*) a matrix of habitat similarity, *iii*) a matrix of spatial connectivity  
155 among their ranges, and *iv*) a phylogenetic distance matrix. Then, we used generalized  
156 partial matrix regression to model the similarity in species occurrences as a function of  
157 these four matrices (Fig.1b). We used this workflow to explore the factors involved in  
158 the configuration of *Carabus* faunas either at the European scale (i.e. co-occurrence  
159 patterns of European *Carabus* species across the delimited regions, hereafter “regional

160 scale”) and independently (i.e. within regions co-occurrence patterns of *Carabus*  
161 species within each delimited region, “hereafter sub-regional scale”). Finally, we also  
162 applied ancestral range estimation analysis in order to identify the time period from  
163 which ancestral areas are estimated with less uncertainty. By doing so, we aimed to  
164 detect important historical periods contributing to the regional organization of  
165 *Carabus* lineages.

166  
167 The interpretation of the joint and independent effects of explanatory matrices can  
168 shed light on the different processes configuring regional faunas (see Fig.1a). In that  
169 way, if niche similarities (i.e. represented by the climatic and habitat similarity  
170 matrices) and phylogenetic distances altogether explained the regional co-occurrence  
171 of species, then this could be interpreted as indicative of constrained niche evolution  
172 (or a tendency to resemble ancestral niches) in shaping regional faunas (Fig.1a.i).  
173 However, if spatial connectivity also accounted for part of this co-occurrence, this  
174 would indicate that this niche conservatism pattern can be caused by geographical  
175 constraints (Fig.1a.ii). Further, the independent effects of niche similarities together  
176 with spatial connectivity can be more likely the consequence of a convergence of  
177 climatic niches due to geographical isolation (Fig.1a.iii). Whereas the effects of  
178 connectivity and phylogeny would be indicative of a primacy of intra-regional  
179 speciation driven by geographical barriers. Niche similarities alone would point to an  
180 unconstrained niche evolution shaping regional faunas, while phylogeny alone would  
181 indicate a primacy of geographically unconstrained intra-regional speciation events.  
182 Finally, either a *cul-de-sac* effect (i.e. the accumulation of species in past climatic  
183 refugia) or a primacy of vicariant speciation events could lead to the existence of  
184 independent effects of connectivity and regional co-occurrence (Fig.1a.iv).

185

### 186 **Identification of regional species pools**

187 We took advantage of community detection analysis —borrowed from network  
188 theory— to identify *Carabus* regional species pools in Europe. To do so, we derived a  
189 bipartite network from the presence-absence matrix, where species and grid cells  
190 constitute two disjoint sets of nodes that are mutually connected according to the  
191 presence of species in grid cells (e.g. Calatayud et al. 2016a). Then, we conducted a

192 modularity analysis using the index proposed by Barber (2007) and the Louvain  
193 algorithm (Blondel et al. 2008, as implemented in the Matlab function “Gen Louvain”,  
194 available at <http://netwiki.amath.unc.edu>; Mucha et al. 2010) to identify the optimal  
195 modular structure of the bipartite network. That is, the optimal groups of grid cells  
196 that show similar *Carabus* species composition together with their associated species  
197 (i.e. network modules). We performed a heuristic search for an optimal solution,  
198 where this analysis was repeated iteratively to obtain 100 different modular solutions,  
199 retaining the one that showed the highest modularity value. This optimal solution was  
200 used to conduct all subsequent analyses, although all the solutions were qualitatively  
201 similar. We evaluated the statistical significance of the modules by comparing its  
202 associated modularity value to a null distribution of values ( $n = 100$ ) where the original  
203 presence absence matrix was randomized using the independent swap algorithm (a  
204 fixed-fixed null model implemented in the R package “picante”, Kembel et al. 2010). In  
205 order to detect potential sub-modules nested within modules (i.e. sub-regional species  
206 pools within regional species pools), we derived a new bipartite network from each of  
207 the modules previously identified in the optimal solution, and applied the procedure  
208 described above in each case.

209

210 It is important to note that despite species and grid cells were assigned to just one  
211 module, they could participate with different degrees in other modules. For example,  
212 despite most species in a grid cell will belong to the same module the cell does, this  
213 cell could also hold species of other modules. Similarly, although a species will mostly  
214 be present in cells assigned to its module, it may also occur in cells from other  
215 modules. Thus, we calculated the degree of module affinity for each node of the  
216 bipartite network as the proportion of links shown by a given node within its module  
217 divided by the total number of its links (note that this index is related to the inter-  
218 modular participation index of Guimera and Amaral 2005). Species with low module  
219 affinity will tend to be widespread throughout Europe, belonging to different regional  
220 species pools. While species with high module affinity will be mainly distributed within  
221 their corresponding modules (highly endemic species). On the other hand, grid cells  
222 with low module affinity may represent transition zones between regions.

223



224

## 225 **Assessing the determinants of regional species pools**

226 In order to disentangle the determinants of the current configuration of *Carabus*  
227 faunas in Europe, we first generated a species-per-module matrix, where each entry  
228 of the matrix represents the percentage of the distributional range of a certain species  
229 that lies in a given module. Then we derived a co-occurrence pairwise similarity matrix  
230 from the former matrix using the Schoener index (Schoener 1970). This index describes  
231 the degree of overlap between species pairs according to their distributions  
232 throughout the modules (see Krasnov et al. 2012) for a previous application to similar  
233 purposes). It ranges from 0 (i.e. complete lack of overlap) to 1 (i.e. identical pattern of  
234 module distribution). Note that this similarity matrix reflects the co-occurrence  
235 similarities at regional scale, ignoring lower-scaled distributional patterns (i.e. two  
236 species may have identical regional distribution but differ in the grid cell they are  
237 present). The resultant co-occurrence pairwise similarity matrix was used as  
238 dependent variable. We generated four different pairwise similarity matrices to be  
239 used as explanatory variables. Two of them to account for environmental factors,  
240 namely (i) a climatic-niche similarity matrix, and (ii) a habitat similarity matrix; and the  
241 other two for geographical and evolutionary factors, respectively: (iii) a spatial-  
242 connectivity matrix, and (iv) a phylogenetic distance matrix.

243

244 *i) Climatic-niche similarity matrix.* We characterized the climatic niche of each *Carabus*  
245 species in the dataset following the approach proposed by Broennimann et al. (2012).  
246 We selected six bioclimatic variables to account for the main water and energy aspects  
247 of climate –namely mean annual temperature, temperature of the warmest quarter,  
248 temperature of the driest quarter, total annual precipitation, total precipitation of the  
249 warmest quarter and total precipitation of the driest quarter– and altitudinal range to  
250 account for the effects of mesoclimatic gradients within each grid cell. These variables  
251 may be among the main determinants of the distribution of *Carabus* species diversity  
252 within Europe (see Calatayud et al. 2016b). We conducted a principal components  
253 analysis (PCA) on these variables to obtain a bidimensional climatic space defined by  
254 the two main axes (81.4% of the variance, Fig.S2). Finally, we divided this climatic  
255 space into 100 grid cells, and applied kernel smoothers to the species occurrence



256 densities in the gridded climatic space to calculate niche overlap between species  
257 using the Schoener index (see above). Note that the kernel density function requires at  
258 least five occurrences of the species, hence species occurring in less than five grid cells  
259 were excluded from subsequent analysis ( $n = 12$ ).

260

261 *ii) Habitat similarity matrix.* The distribution of *Carabus* species may also be shaped by  
262 their forest preferences (Turin et al. 2003). Thus, we made use of information relative  
263 to the type of vegetation where each species tends to occur in order to characterize  
264 their environmental niche. We calculated the fraction of each species' distributional  
265 range laying within each vegetation category, according to 10 vegetation categories  
266 derived from MODIS dataset (Evergreen broadleaf forest, deciduous needle leaf forest,  
267 deciduous broadleaf forest, mixed forest, closed shrub lands, open shrub lands, woody  
268 savannas, savannas and grasslands). Then, we computed pairwise similarities in the  
269 preference to different vegetation types using the Schoener index (see above).

270

271 *iii) Spatial connectivity matrix.* To evaluate the potential influence of dispersal barriers  
272 on the current distribution of *Carabus* species we first created a dispersal-cost surface  
273 by weighting each pixel in the study area according to both its topography (in this case,  
274 slope) and the presence of water bodies. Slope values ranging from 0 to 100% at each  
275 pixel and were determined from GTOPO30 altitudinal data using the GRASS tool  
276 `r.slope` (GRASS Development Team 2017). Water bodies from Nature Earth were assigned  
277 arbitrary values of friction to the dispersal of *Carabus* species, namely 30% for pixels  
278 containing rivers and lakes and 99% for pixels that lay on sea water masses (note that  
279 *Carabus* species show hydrophilic adaptations). Then, the connectivity between all  
280 pairs of cells was calculated as least-cost path over the dispersal-cost surface that  
281 connect both cells, using the “`gdistance`” R package (van Etten 2015). Finally, the spatial  
282 connectivity between two species' distributional ranges was estimated as the average  
283 distance among all grid cells within the range of each species. Average distances were  
284 preferred over absolute least-cost distances to avoid disproportionate differences in  
285 spatial connectivity between overlapping and non-overlapping distributional ranges.

286

287 *iv) Phylogenetic distance matrix.* To unravel the evolutionary history of *Carabus* lineage  
288 and the importance of evolutionary processes in determining the formation of *Carabus*  
289 species pool, we reconstructed a species-level time-calibrated molecular phylogeny  
290 including 89 species. We used a maximum-likelihood inference based on ten DNA  
291 markers (see Appendix S3 for full details). We used taxonomic information and  
292 phylogenetic uncertainty methods (Rangel et al. 2015) to place species lacking  
293 molecular information into the phylogeny (see Appendix S3). Thus, we derived 100  
294 different phylogenetic hypotheses from the maximum-likelihood phylogeny, by  
295 randomly inserting missing species within their most derived consensus clade based on  
296 taxonomic knowledge.

297

298 We used multiple regression on distance matrices and variance partitioning to  
299 disentangle the relative importance of climatic niche, habitat preferences, dispersal  
300 barriers and evolutionary history in determining *Carabus* species pools in Europe. First,  
301 we conducted single regressions between the co-occurrence pairwise similarity matrix  
302 and each of the four explanatory matrices described above to seek for significant  
303 associations between the variables. Given that the distribution of co-occurrence  
304 pairwise values was rather bimodal with modes at 0 and 1, respectively, we set a  
305 binomial family for error distribution and “logit” as the link function (see Ferrier et al.  
306 2007 and Calatayud et al. 2016a for a similar approach). To assess for significance, we  
307 randomized the original species per module matrix using the independent swap  
308 algorithm (see above) to derive 999 null occurrence pairwise similarity matrices. Then,  
309 we fitted single regressions between the null occurrence pairwise similarity matrices  
310 and each of the explanatory similarity matrices, and considered a variable to have a  
311 significant effect when the regression based on observed data explained a higher  
312 deviance than 99% of the null regressions. In the case of phylogenetic pairwise  
313 distances we repeated this procedure for each phylogenetic hypothesis to take into  
314 account phylogenetic uncertainties, applying the same criterion for significance.  
315 Finally, we retained those variables that showed significant associations with the co-  
316 occurrence pairwise similarity matrix, and conducted partial multiple regression  
317 (Legendre and Legendre 2012) on distance matrices to explore patterns of covariation  
318 among niche similarities (i.e. climatic and habitat similarity matrices) dispersal barriers

319 and phylogenetic history. We repeated this whole procedure for each module  
320 independently, to further explore the determinants of *Carabus* species co-occurrence  
321 into submodules.

322

### 323 **Ancestral range estimation**

324 Probabilistic models of geographic range evolution have proven to be of great utility to  
325 deal with historical biogeographical questions (see Ronquist and Sanmartín 2011 and  
326 references therein). Here we used these models to try to unravel whether, as  
327 predicted by Wallace (1876), deep historical signals were eroded by Pleistocene  
328 glaciations in the configuration of European *Carabus* faunas. We used a maximum  
329 likelihood approach for inferring geographical range evolution implemented in the R  
330 package BioGeoBears (Matzke 2014), using independently each one of the 100  
331 phylogenetic hypotheses created before. BioGeoBears fits a variety of models that  
332 differ in their rates and/or types of dispersal, extinction, sympatric speciation,  
333 vicariance and founder event speciation. We fitted the six available models (DEC,  
334 DEC+J, DIVALIKE, DIVALIKE+J, BAYAREALIKE, BAYAREALIKE+J, see Matzke 2013)  
335 comparing their informative capacity through the Akaike information criterion (AIC).  
336 Species ranges were here coded as present/absent in each region detected in the  
337 former network analyses.

338

339 The estimation of ancestral ranges usually tends to be more ambiguous in deeper  
340 nodes of the phylogeny, as the potential lability of geographical ranges would tend to  
341 blur deep time signals (Losos and Glor 2003). Yet, if the Pleistocene glacial periods had  
342 important effects in the distribution of species it could be expected that ancestral  
343 range estimations will begin to be more accurate around the Pleistocene (that is, pre-  
344 Pleistocene signals on distributional range evolution will be eroded). To explore this we  
345 attended to potential changes in the relationship between node age and the marginal  
346 probability of the single most-probable ancestral state at each internal node. We  
347 obtained these probabilities from the best model among the six geographical range  
348 evolution models in BioGeoBears (see above) and in each of the phylogenetic  
349 hypotheses used. Then, general additive mixed models (GAMMs) were fitted to the  
350 node marginal probability as a function of node age, including the phylogenetic

351 hypothesis as a random factor. Further, in case we found different best models in  
352 different phylogenetic hypotheses we also included a fixed variable with the model  
353 type. Finally, we also carried out generalized linear mixed models (GLMMs) using a  
354 piecewise regression procedure to assess for a shift in the relationship between  
355 marginal probability and node age. The breakpoint in the piecewise regression was  
356 assessed by including the breakpoint as a new parameter in the GLMM and then  
357 minimizing the deviance of the fitted model using the function “optimize” in the R  
358 package lme4 (Bates et al. 2014). Finally, we used AICc to compare the models with  
359 and without breakpoint. In both cases we used a binomial family and a loglink  
360 function, since the marginal probabilities of the nodes vary between zero and one. All  
361 analyses were carried out in R (R core team 2015),: GAMM with the package gamm4  
362 (Wood and Scheipl 2014), GLMM with lme4 (Bates et al. 2014) and AICc with  
363 AICcmodavg (Mazerolle 2011).

364

## 365 **Results**

### 366 **Identification of regional faunas**

367 The *Carabus* occurrence network was significantly modular ( $M=0.385$ ,  $p=0.01$ ), dividing  
368 Europe in seven modules that group zoogeographically distinct regions with their  
369 associated faunas; that is, different regional species pools (Figs. 2 and S1). Further, all  
370 modules but module 2 showed a significant sub-modular structure, presenting a  
371 decrease in modularity with latitude (mean  $M=0.316$ , ranging from 0.154 to 0.468; all  
372  $p$ -values  $< 0.05$ , see Table S1). Module 1 holds 21 species mainly living in Southwestern  
373 Palearctic (Iberian Peninsula, North of Africa, Balearic Islands, Corsica, Sardinia and the  
374 western half of Sicilia). This module was subdivided into four submodules. Module 2  
375 only groups two species which are endemic of Crete. Module 3 identifies an East  
376 Mediterranean region including the Italic Peninsula, part of Greece and Turkey. This  
377 module holds 18 species and was subdivided into five submodules. Module 4 depicts a  
378 Central European region embracing the Alps and Carpathian Mountains, as well as  
379 Central European plains. This module is the richest one, with forty-nine *Carabus*  
380 species, and was split into 4 submodules. Module 5 and module 6 correspond with  
381 northern regions and are the poorest ones, holding ten species each. The former  
382 expands from Iceland and the British Isles almost to the Ural Mountains. The latter

383 includes The Ural Mountains and expands to the easternmost zone of the study area.  
384 Both modules were divided into 3 submodules. Finally, module 7 includes 21 species  
385 and embraces a south-eastern central European region expanding from the Carpathian  
386 Mountains to the south Ural Mountains. This module was split into 3 submodules.

387

388 The transition zones between regions appear to be associated with geographical  
389 barriers such as the Pyrenees, Alps, Carpathian and Ural Mountains, as well as the  
390 Bosphorus strait (Fig. 2c). Further, we also found a transition zone running through  
391 Central Europe in a west-to-east belt, separating southern and northern regions.  
392 Interestingly, this transition zone closely follows the southern limits of the ice sheet at  
393 the Last Glacial Maximum (LGM), suggesting a link between the configuration of  
394 *Carabus* regional faunas and Pleistocene glacial conditions.

395

396

### 397 **Correlates of regional co-occurrence**

398 Matrix regressions showed that both environmental niche similarity (i.e. climate and  
399 habitat) and spatial connectivity were significantly related to species co-occurrence in  
400 regions and sub-regions ( $p < 0.01$ ). In contrast, evolutionary relatedness was not related  
401 with regional co-occurrence, as phylogenetic distances did not show a significant  
402 relationship at  $p > 0.01$  for any single phylogenetic hypothesis. Environmental niche  
403 similarity was the best predictor of co-occurrence in both regions and sub-regions,  
404 although its effects were stronger when predicting the co-occurrence into sub-regions  
405 (Fig. 3). Spatial connectivity had stronger effects when predicting the co-occurrence  
406 into regions relative to sub-regions, where its effect mostly overlapped with that of  
407 environmental niche. The relative importance of these two sets of factors showed a  
408 clear latitudinal trend. The effects of connectivity were stronger in southern regions  
409 (i.e. modules 1 and 3), which is not surprising given the more complex orography of  
410 these regions. But importantly, although niche similarity was the best predictor of co-  
411 occurrence in all cases, its effects became more evident towards northern regions.  
412 Indeed, niche similarities and spatial connectivity were significant predictors of the co-  
413 occurrence into sub-regions in all regional pools except the two northern ones (Table  
414 S2). Only niche similarities (mainly climate) showed significant effects in these two

415 modules (i.e. 5 and 6), as expected if the species in these regional pools colonized the  
416 northern regions only recently, and were geographically sorted according to current  
417 climate.

418

#### 419 **Ancestral range estimation**

420 BAYAREALIKE+J model was the best supported by data in 59% of the phylogenetic  
421 hypotheses, followed by DEC+J and DEC, which were the best in 23 and 18% of the  
422 hypotheses, respectively (Table 1). Interestingly, the BAYAREALIKE+J model does not  
423 account for vicariant cladogenetic events. Rather, it considers founder effect  
424 speciation, which could be seen as a signal of Pleistocene glaciations promoting  
425 speciation in glacial refugia (i.e. acting as islands) and eroding the ancestors' ranges.  
426 Indeed, according to this model the range contraction parameter had the highest  
427 estimate (Table 1). This parameter was however of little importance in the other two  
428 models, which accounted for vicariant events in both cases. Regardless the  
429 biogeographical model used, GAMM results showed that node marginal probability of  
430 the most probable state increased as expected towards younger nodes ( $P < 0.01$ ,  $R^2$   
431  $= 0.34$ ). However, this increase became abrupt coinciding with the beginning of the  
432 Pleistocene – which started around 2.59 Mya.– (Fig.4). Indeed, we found that the  
433 GLMM including the breakpoint was better in terms of AICc (AICc weight for the model  
434 including the breakpoint = 1), and that the relationship between state probability and  
435 node age changed at 2.47 Mya. (confidence interval at 95% = 2.23, 2.73). This points to  
436 the signal left by the Pleistocene on the configuration of European *Carabus* faunas.  
437 These results were confirmed using different approaches (see Appendix S4).

438

439

#### 440 **Discussion**

441 More than 140 years ago, Wallace (1876) foresaw that the influence of Pleistocene  
442 glaciations on the distribution of diversity had been strong enough so as to erode the  
443 imprint of previous events. Our results confirm Wallace's thoughts, showing a  
444 remarkable coincidence between the distribution of the ice sheet at the Last Glacial  
445 Maximum and the current configuration and evolutionary structure of European  
446 *Carabus* Faunas. There is a close spatial relationship between the southern limits of the

447 area glaciated at LGM, and the transition zone separating the southern and northern  
448 regions identified by our analyses. Indeed, this border also coincides with the line  
449 identified by Calatayud et al. (2016b), where the relationship between *Carabus* species  
450 richness and current climate changes in shape and strength (Fig. 2). Thus, it seems that  
451 the climate changes underwent during the Pleistocene not only shape local diversity  
452 patterns (e.g. Svenning and Skov 2007, Araujo et al. 2008, Hortal et al. 2011), but they  
453 have also left a strong imprint on the geographical structure of species composition at  
454 a regional scale. Accordingly, the species from the northernmost region (module 5)  
455 show the lowest level of endemism (Fig. S2, as expected for regional faunas composed  
456 of species that have recently colonized the north of Europe from southern glacial  
457 refugia; Araujo et al. 2008, Calatayud et al. 2016b). In fact, although these species are  
458 widely distributed across southern Europe, all of their ranges only overlap near to the  
459 northern Carpathian Mountains, an area that has been shown to be a glacial refugia  
460 for some *Carabus* species (Homburg et al. 2013, Fig. S3). Additionally, the decrease in  
461 modularity values with latitude also points to a lesser geographical structure of  
462 northern assemblages, which can be interpreted as the result of a post-glacial  
463 colonization.

464

465 Besides the Pleistocene effects in the definition and geographical structure of regional  
466 pools of species, we also found evidence of the imprint of this geological period on the  
467 processes configuring the distribution of *Carabus* faunas. The generally strong  
468 relationship between regional patterns of co-occurrence and both niche similarities  
469 and spatial connectivity shows that co-occurring species tend to have similar realized  
470 environmental niches and that also tend to be geographically constrained by the same  
471 dispersal barriers. This latter result was expected, given the low dispersal capacity of  
472 *Carabus* species (see Turin et al. 2003), which is likely to be behind the spatial  
473 coincidence of the zones of transition between regional faunas and geographical  
474 barriers. Perhaps more unexpected is the relationship of regional co-occurrence and  
475 niche similarities without any significant phylogenetic effect. This implies that the  
476 geographical configuration of barriers to dispersal has restricted species within regions  
477 of similar climate, rather than climatic-niche conservatism constraining their co-  
478 occurrences. These results point to that *Carabus* niche evolution is, to some extent,



479 evolutionary unconstrained, which is congruent with the high adaptation capacity of  
480 insects in general (e.g. Overgaard and Sørensen 2008). Going further, this questions to  
481 what extent the observed species' regional occurrence is the consequence of their  
482 environmental niche and not the other way around (see Hortal et al. 2012, Wüest et al.  
483 2015).

484  
485 Whatever the origin of the relationship between species occurrence and  
486 environmental conditions, which is certainly true is that its strength changes among  
487 regions. These changes follow a latitudinal gradient in the importance of  
488 environmental niche similarities. In northern regions, the similarity in the realized  
489 niche seems to be stronger related to the occurrence into sub-regions than in the  
490 south. This might be a direct consequence of the processes that determine regional  
491 pools being dependent on the particular history of each region (Ricklefs 2015). These  
492 findings are also congruent with the effects of post-glacial colonization, where  
493 formerly glaciated areas show a clear sorting of species northwards due to low time for  
494 dispersal (Svenning and Skov 2007). This contrasts with southern regions, where  
495 climate has been milder and more stable and the species have had more time to  
496 diversify. This suggests that species' geographical arrangement in southern latitudes is  
497 more likely the result of historical contingency rather than environmental preferences  
498 (Hortal et al. 2011, Calatayud et al. 2016b).

499  
500 The lack of relationship between the phylogenetic distances among *Carabus* species  
501 and their regional co-occurrence can be the outcome of either a generalized  
502 preponderance of vicariant events and/or a “cul-de-sac effect” (O'Regan 2008). The  
503 former will more likely imply that the generation of the dispersal barriers that shaped  
504 the regions will also promote the geographical split of many lineages and subsequent  
505 allopatric speciation events (Weeks et al. 2016). Yet, the formation of the geographical  
506 accidents associated to the delimitation of *Carabus* regions largely predates the origin  
507 of the genus (see Beccaluva et al. 1998, Deuve et al. 2012). On the other hand, a  
508 generalized dispersion into climatic refugia, together with a subsequent stagnancy  
509 within them (i.e. a “cul-de-sac” effect) may also produce the observed mixing of  
510 unrelated lineages into regions. Although it is difficult to distinguish between both

511 processes, we believe it is more plausible to think that southern regions have  
512 accumulated unrelated species while acting as glacial refugia, whereas northern  
513 regions were recolonized by unrelated species with similar environmental niches ---or  
514 simply with higher dispersal capacity (see above).

515

516 In agreement with this idea, the model of ancestral range estimation that is best  
517 supported by the data does not include vicariant events. On the contrary, this model  
518 takes into account founder speciation events, a process typical from islands (Provine  
519 1989). This could be interpreted on the light of southern regions acting as islands  
520 during the different Pleistocene glacial maxima. Should this be true, a temporal signal  
521 of this period on the spatial organization of *Carabus* lineages should be evident in their  
522 phylogeny. We found such signal on the relationship between node maximum  
523 probability state and node age. Indeed, the striking coincidence between the  
524 breakpoint where this relationship becomes steeper and the beginning of the  
525 Pleistocene argues in favour of the imprint of this epoch on the configuration of  
526 *Carabus* regional faunas. We obtained similar results using several other approaches  
527 (Appendix S4), supporting the notion that the current regional organization of *Carabus*  
528 species and lineages has its very roots at the beginning of the Pleistocene. This contrasts  
529 with ancestral range estimations for clades inhabiting areas that were never glaciated,  
530 where more ancient signals were found in the spatial sort of lineages (Condamine et al.  
531 2015, Economo et al. 2015, Tänzler et al. 2016, Toussaint and Balke 2016). It thus  
532 seems that the repeated advances and retreats of ice sheets during this geological  
533 period produced the repeated cycles of retreat to southern regions and advance  
534 towards northern regions of *Carabus* species, a hustle-and-bustle process that  
535 ultimately led to the observed mixing of unrelated lineages.

536

537 In sum, our results provide solid arguments in favour of the importance of Pleistocene  
538 glaciations along with geographical barriers in structuring the regional faunas of this  
539 group. On the one hand, European *Carabus* faunas are primarily delimited by the  
540 location of the southern limit of the ice sheet at LGM, which separates two large  
541 regions that differ not only in species composition, but also in the processes underlying  
542 the spatial organization of these species. On the other hand, the phylogenetic

543 structure of these faunas coincides with the beginning of the Pleistocene. This not only  
544 implies that the geographical distribution of species and lineages is deeply shaped by  
545 past climates, but also that the ecological processes (Naeslund and Norberg 2006,  
546 Madrigal et al. 2016) and evolutionary mechanisms ( Wüest et al. 2015, Calatayud et  
547 al. 2016a) that are dependent on regional species pools may be profoundly affected by  
548 the history of Earth climates. It is therefore essential to take into account past  
549 historical events while trying to understand, not only current diversity patterns and the  
550 processes behind them, but also processes and patterns occurring at local scales.

551

## 552 **References**

- 553 1. Araújo, M. B., D. Nogués-Bravo, J. A. F. Diniz-Filho, A. M. Haywood, P. J. Valdes,  
554 and C. Rahbek. 2008. Quaternary climate changes explain diversity among reptiles  
555 and amphibians. *Ecography* **31**:8–15.
- 556 2. Barber, M. J. 2007. Modularity and community detection in bipartite networks.  
557 *Physical Review E* **76**:066102.
- 558 3. Barnes, I., P. Matheus, B. Shapiro, D. Jensen, and A. Cooper. 2002. Dynamics of  
559 Pleistocene population extinctions in Beringian brown bears. *Science* **295**:2267–  
560 2270.
- 561 4. Bates, D., M. Maechler, B. Bolker, S. Walker, et al. 2014. lme4: Linear mixed-  
562 effects models using Eigen and S4. R package version **1**.
- 563 5. Beccaluva, L., M. Shallo, M. Coltorti, I. Premti, and F. Siena. 1998. *Encyclopedia of*  
564 *European and Asian Regional Geology*. Springer.
- 565 6. Blondel, V. D., J.-L. Guillaume, R. Lambiotte, and E. Lefebvre. 2008. Fast unfolding  
566 of communities in large networks. *Journal of Statistical Mechanics* **2008**:P10008.
- 567 7. Broennimann, O., M. C. Fitzpatrick, P. B. Pearman, B. Petitpierre, L. Pellissier, N. G.  
568 Yoccoz, W. Thuiller, M.-J. Fortin, C. Randin, N. E. Zimmermann, et al. 2012.  
569 Measuring ecological niche overlap from occurrence and spatial environmental  
570 data. *Global Ecology and Biogeography* **21**:481–497.
- 571 8. Calatayud, J., J. L. Hórreo, J. Madrigal-González, A. Migeon, M. Á. Rodríguez,  
572 S. Magalhães, and J. Hortal. 2016a. Geography and major host evolutionary  
573 transitions shape the resource use of plant parasites. *Proceedings of the National*  
574 *Academy of Sciences USA* **113**:9840–9845.
- 575 9. Calatayud, J., J. Hortal, N. G. Medina, H. Turin, R. Bernard, A. Casale, V. M. Ortuño,  
576 L. Penev, and M. Á. Rodríguez. 2016b. Glaciations, deciduous forests, water  
577 availability and current geographical patterns in the diversity of European *Carabus*  
578 species. *Journal of Biogeography* **43**:2343–2353.
- 579 10. Cardillo, M. 2011. Phylogenetic structure of mammal assemblages at large  
580 geographical scales: linking phylogenetic community ecology with macroecology.  
581 *Philosophical Transactions of the Royal Society of London B* **366**:2545–2553.
- 582 11. Channan, S., K. Collins, and W. Emanuel. 2014. Global mosaics of the standard  
583 MODIS land cover type data. University of Maryland and the Pacific Northwest  
584 National Laboratory, College Park, Maryland, USA .

- 585 12. Colwell, R. K., and T. F. Rangel. 2009. Hutchinson's duality: the once and future  
586 niche. *Proceedings of the National Academy of Sciences USA* **106**:19651–19658.
- 587 13. Condamine, F. L., E. F. Toussaint, A.-L. Clamens, G. Genson, F. A. Sperling, and G. J.  
588 Kergoat. 2015. Deciphering the evolution of birdwing butterflies 150 years after  
589 Alfred Russel Wallace. *Scientific Reports* **5**:11860.
- 590 14. Crisp, M. D., S. A. Trewick, and L. G. Cook. 2011. Hypothesis testing in  
591 biogeography. *Trends in Ecology and Evolution* **26**:66–72.
- 592 15. Deuve, T., A. Cruaud, G. Genson, and J.-Y. Rasplus. 2012. Molecular systematics  
593 and evolutionary history of the genus *Carabus* (Col. Carabidae). *Molecular*  
594 *Phylogenetics and Evolution* **65**:259–275.
- 595 16. Ebach, M.C. 2015. *Origins of Biogeography*. Springer, New York.
- 596 17. Economo, E. P., E. M. Sarnat, M. Janda, R. Clouse, P. B. Klimov, G. Fischer, B. D.  
597 Blanchard, L. N. Ramirez, A. N. Andersen, M. Berman, et al. 2015. Breaking out of  
598 biogeographical modules: range expansion and taxon cycles in the hyperdiverse  
599 ant genus *Pheidole*. *Journal of Biogeography* **42**:2289–2301.
- 600 18. Ehlers, J., and P. L. Gibbard. 2004. Quaternary glaciations—extent and chronology:  
601 part I: Europe. Elsevier.
- 602 19. Ferrier, S., G. Manion, J. Elith, and K. Richardson. 2007. Using generalized  
603 dissimilarity modelling to analyse and predict patterns of beta diversity in regional  
604 biodiversity assessment. *Diversity and Distributions* **13**:252–264.
- 605 20. Gouveia, S. F., J. Hortal, M. Tejedó, H. Duarte, F. A. Cassemiro, C. A. Navas, and  
606 J. A. F. Diniz-Filho. 2014. Climatic niche at physiological and macroecological  
607 scales: the thermal tolerance–geographical range interface and niche  
608 dimensionality. *Global Ecology and Biogeography* **23**:446–456.
- 609 21. GRASS Development Team, 2017. Geographic Resources Analysis Support System  
610 (GRASS GIS) Software, Version 7.2. Open Source Geospatial Foundation.  
611 <http://grass.osgeo.org>.
- 612 22. Guimerà, R., and L. A. N. Amaral. 2005. Functional cartography of complex  
613 metabolic networks. *Nature* **433**:895–900.
- 614 23. Hewitt, G. M. 1999. Post-glacial re-colonization of European biota. *Biological*  
615 *Journal of the Linnean Society* **68**:87–112.
- 616 24. Hijmans, R. J., S. E. Cameron, J. L. Parra, P. G. Jones, and A. Jarvis. 2005. Very high  
617 resolution interpolated climate surfaces for global land areas. *International*  
618 *Journal of Climatology* **25**:1965–1978.
- 619 25. Holt, B. G., J.-P. Lessard, M. K. Borregaard, S. A. Fritz, M. B. Araújo, D. Dimitrov, P.-  
620 H. Fabre, C. H. Graham, G. R. Graves, K. A. Jønsson, et al. 2013. An update of  
621 Wallace's zoogeographic regions of the world. *Science* **339**:74–78.
- 622 26. Homburg, K., C. Drees, M. M. Gossner, L. Rakosy, A. Vrezec, and T. Assmann. 2013.  
623 Multiple glacial refugia of the low-dispersal ground beetle *Carabus irregularis*:  
624 molecular data support predictions of species distribution models. *PloS One*  
625 **8**:e61185.
- 626 27. Hortal, J., P. De Marco Jr, A. Santos, and J. A. F. Diniz-Filho. 2012. Integrating  
627 biogeographical processes and local community assembly. *Journal of*  
628 *Biogeography* **39**:627–628.
- 629 28. Hortal, J., J. A. F. Diniz-Filho, L. M. Bini, M. Á. Rodríguez, A. Baselga, D. Nogués-  
630 Bravo, T. F. Rangel, B. A. Hawkins, and J. M. Lobo. 2011. Ice age climate,

- 631 evolutionary constraints and diversity patterns of European dung beetles. *Ecology*  
632 *Letters* **14**:741–748.
- 633 29. Hortal, J., J. M. Lobo, and A. Jiménez-Valverde. 2012. Basic questions in  
634 biogeography and the (lack of) simplicity of species distributions: putting species  
635 distribution models in the right place. *Natureza & Conservação* **10**:108–118.
- 636 30. Hortal, J., N. Roura-Pascual, N. Sanders, and C. Rahbek. 2010. Understanding  
637 (insect) species distributions across spatial scales. *Ecography* **33**:51.
- 638 31. Johnson, N. K., C. Cicero, and K. Shaw. 2004. New mitochondrial DNA data affirm  
639 the importance of Pleistocene speciation in North American birds. *Evolution*  
640 **58**:1122–1130.
- 641 32. Kembel, S. W., P. D. Cowan, M. R. Helmus, W. K. Cornwell, H. Morlon, D. D.  
642 Ackerly, S. P. Blomberg, and C. O. Webb. 2010. Picante: R tools for integrating  
643 phylogenies and ecology. *Bioinformatics* **26**:1463–1464.
- 644 33. Krasnov, B. R., M. A. Fortuna, D. Mouillot, I. S. Khokhlova, G. I. Shenbrot, and  
645 R. Poulin. 2012. Phylogenetic signal in module composition and species  
646 connectivity in compartmentalized host-parasite networks. *The American*  
647 *Naturalist* **179**:501–511.
- 648 34. Legendre, P., and L. F. Legendre. 2012. *Numerical ecology*. Elsevier.
- 649 35. Losos, J. B., and R. E. Glor. 2003. Phylogenetic comparative methods and the  
650 geography of speciation. *Trends in Ecology and Evolution* **18**:220–227.
- 651 36. Madrigal-González, J., P. Ruiz-Benito, S. Ratcliffe, J. Calatayud, G. Kändler,  
652 A. Lehtonen, J. Dahlgren, C. Wirth, and M. A. Zavala. 2016. Complementarity  
653 effects on tree growth are contingent on tree size and climatic conditions across  
654 Europe. *Scientific Reports* **6**:32233.
- 655 37. Matzke, N. J., 2013. BioGeoBEARS: BioGeography with Bayesian (and Likelihood)  
656 Evolutionary Analysis in R Scripts. University of California, Berkeley, Berkeley, CA.  
657 <http://CRAN.R-project.org/package=BioGeoBEARS>.
- 658 38. Matzke, N. J. 2014. Model selection in historical biogeography reveals that  
659 founder-event speciation is a crucial process in island clades. *Systematic Biology*  
660 **63**:51–70.
- 661 39. Mazerolle, M. J. 2011. AICcmodavg: model selection and multimodel inference  
662 based on (Q) AIC (c). R package version **1**.
- 663 40. Medina, N. G., B. Albertos, F. Lara, V. Mazimpaka, R. Garilleti, D. Draper, and  
664 J. Hortal. 2014. Species richness of epiphytic bryophytes: drivers across scales on  
665 the edge of the Mediterranean. *Ecography* **37**:80–93.
- 666 41. Mittelbach, G. G., and D. W. Schemske. 2015. Ecological and evolutionary  
667 perspectives on community assembly. *Trends in Ecology and Evolution* **30**:241–  
668 247.
- 669 42. Mucha, P. J., T. Richardson, K. Macon, M. A. Porter, and J.-P. Onnela. 2010.  
670 Community structure in time-dependent, multiscale, and multiplex networks.  
671 *Science* **328**:876–878.
- 672 43. Naeslund, B., and Norberg, J. 2006. Ecosystem consequences of the regional  
673 species pool. *Oikos*, **115**:504-512.
- 674 44. O’Regan, H. J. 2008. The Iberian Peninsula—corridor or cul-de-sac? Mammalian  
675 faunal change and possible routes of dispersal in the last 2 million years.  
676 *Quaternary Science Reviews* **27**:2136–2144.

- 677 45. Overgaard, J., and J. G. Sørensen. 2008. Rapid thermal adaptation during field  
678 temperature variations in *Drosophila melanogaster*. *Cryobiology* **56**:159–162.
- 679 46. Provine, W. B., 1989. Founder effects and genetic revolutions in microevolution  
680 and speciation: an historical perspective. Pp. 43–76 in L. Val Giddings and K. Y.  
681 Kaneshiro, editors. *Genetics, speciation, and the founder principle*. Oxford  
682 University Press.
- 683 47. R Core Team, 2015. R: A Language and Environment for Statistical Computing. R  
684 Foundation for Statistical Computing, Vienna, Austria. <http://www.R-project.org/>.
- 685 48. Rangel, T. F., R. K. Colwell, G. R. Graves, K. Fučíková, C. Rahbek, and J. A. F. Diniz-  
686 Filho. 2015. Phylogenetic uncertainty revisited: Implications for ecological  
687 analyses. *Evolution* **69**:1301–1312.
- 688 49. Ricklefs, R. E. 2008. Disintegration of the ecological community. *The American*  
689 *Naturalist* **172**:741–750.
- 690 50. Ricklefs, R. E. 2011. Applying a regional community concept to forest birds of  
691 eastern North America. *Proceedings of the National Academy of Sciences USA*  
692 **108**:2300–2305.
- 693 51. Ricklefs, R. E. 2015. Intrinsic dynamics of the regional community. *Ecology Letters*  
694 **18**:497–503.
- 695 52. Ricklefs, R. E., and F. He. 2016. Region effects influence local tree species diversity.  
696 *Proceedings of the National Academy of Sciences USA* **113**:674–679.
- 697 53. Ronquist, F., and I. Sanmartín. 2011. Phylogenetic methods in biogeography.  
698 *Annual Review of Ecology, Evolution and Systematics* **42**:441–464.
- 699 54. Rueda, M., M. Á. Rodríguez, and B. A. Hawkins. 2013. Identifying global  
700 zoogeographical regions: lessons from Wallace. *Journal of Biogeography* **40**:2215–  
701 2225.
- 702 55. Schoener, T. W. 1970. Nonsynchronous spatial overlap of lizards in patchy  
703 habitats. *Ecology* **51**:408–418.
- 704 56. Soberón, J. 2007. Grinnellian and Eltonian niches and geographic distributions of  
705 species. *Ecology Letters* **10**:1115–1123.
- 706 57. Svenning, J.-C., W. L. Eiserhardt, S. Normand, A. Ordonez, and B. Sandel. 2015. The  
707 influence of paleoclimate on present-day patterns in biodiversity and ecosystems.  
708 *Annual Review of Ecology, Evolution and Systematics* **46**:551–572.
- 709 58. Svenning, J.-C., and F. Skov. 2007. Could the tree diversity pattern in Europe be  
710 generated by postglacial dispersal limitation? *Ecology Letters* **10**:453–460.
- 711 59. Tänzler, R., M. H. Van Dam, E. F. Toussaint, Y. R. Suhardjono, M. Balke, and  
712 A. Riedel. 2016. Macroevolution of hyperdiverse flightless beetles reflects the  
713 complex geological history of the Sunda Arc. *Scientific Reports* **6**:18793.
- 714 60. Theissingner, K., M. Bálint, K. A. Feldheim, P. Haase, J. Johannesen, I. Laube, and  
715 S. U. Pauls. 2013. Glacial survival and post-glacial recolonization of an arctic–alpine  
716 freshwater insect (*Arcynopteryx dichroa*, *Plecoptera*, *Perlodidae*) in Europe.  
717 *Journal of Biogeography* **40**:236–248.
- 718 61. Toussaint, E. F., and M. Balke. 2016. Historical biogeography of *Polyura* butterflies  
719 in the oriental Palaeotropics: trans-archipelagic routes and South Pacific island  
720 hopping. *Journal of Biogeography* **43**:1560–1572.
- 721 62. Turin, H., L. Penev, A. Casale, E. Arndt, T. Assmann, K. Makarov, D. Mossakowski,  
722 G. Szél, F. Weber, H. Turin, et al., 2003. Species accounts. Pp. 151–284 in H. Turin,



- 723 L. Penev, and A. Casale, editors. The Genus *Carabus* in Europe: A Synthesis.  
724 Pensoft Publishers.
- 725 63. van Etten, J., 2015. gdistance: Distances and Routes on Geographical Grids.  
726 <http://CRAN.R-project.org/package=gdistance>.
- 727 64. Wallace, A. R. 1876. The geographical distribution of animals: with a study of the  
728 relations of living and extinct faunas as elucidating the past changes of the earth's  
729 surface. Cambridge University Press.
- 730 65. Warren, D. L., M. Cardillo, D. F. Rosauer, and D. I. Bolnick. 2014. Mistaking  
731 geography for biology: inferring processes from species distributions. Trends in  
732 Ecology and Evolution **29**:572–580.
- 733 66. Weeks, B. C., S. Claramunt, and J. Cracraft. 2016. Integrating systematics and  
734 biogeography to disentangle the roles of history and ecology in biotic assembly.  
735 Journal of Biogeography **43**:1546–1559.
- 736 67. Wood, S., and F. Scheipl, 2014. gamm4: Generalized additive mixed models using  
737 mgcv and lme4. <http://CRAN.R-project.org/package=gamm4>.
- 738 68. Wüest, R. O., A. Antonelli, N. E. Zimmermann, and H. P. Linder. 2015. Available  
739 climate regimes drive niche diversification during range expansion. The American  
740 Naturalist **185**:640–652.
- 741



742 **Table 1.** Results of the best ancestral range estimation models. d= dispersion, e=  
743 extinction; j= founder speciation. Prop.best = proportion of phylogenetic hypotheses  
744 where a model was the best in terms of AICc. Mean values among different  
745 phylogenetic hypotheses (incl. standard deviation within brackets), are shown for each  
746 parameter.

| Model         | N° param. | d            | e              | j            | Prop. Best |
|---------------|-----------|--------------|----------------|--------------|------------|
| BAYAREALIKE+J | 3         | 0.015(0.001) | 0.063(0.017)   | 0.015(0.005) | 0.59       |
| DEC+J         | 3         | 0.025(0.001) | <0.001(<0.001) | 0.008(0.003) | 0.23       |
| DEC           | 2         | 0.026(0.001) | 0.003(0.001)   | 0            | 0.18       |
| BAYAREALIKE   | 2         | 0.019(0.001) | 0.111(0.006)   | 0            | 0          |
| DIVALIKE      | 2         | 0.031(0.001) | 0.002(0.001)   | 0            | 0          |
| DIVALIKE+J    | 3         | 0.03(0.001)  | 0(0)           | 0.006(0.003) | 0          |

747

748

749 **Figure 1.** Hypothetical examples of the factors configuring regional faunas and work  
750 flow. a) Figure showing four hypothetical processes configuring regional faunas.  
751 Dotted lines depict different regions while colours correspond with different climates.  
752 In each case, the tips of the phylogeny point to regional distribution of the species. b)  
753 Workflow and potential results: 1) Hypothetical results of modularity analysis over the  
754 occurrence network; 2) similarity matrix of occurrence into modules; 3) pairwise  
755 matrix of environmental niche similarities; phylogenetic distances and topographical  
756 connectivity; and 4) hypothetical results and interpretations of a partial matrix  
757 regression on species occurrence similarities as a function of niche similarities,  
758 phylogenetic distances and connectivity.

759

760 **Figure 2.** European *Carabus* regions found by the network community detection  
761 analysis. a) Geographical location of modules (i.e. regions) and submodules. b) Module  
762 simplification of the occurrence network. Circles represent a module, being their size  
763 proportional to the species group within them. Links depict the species shared among  
764 regions, being its width proportional to the number of species. c) Values of module  
765 affinity per grid cell; green colours (i.e. cells with low affinity) identify transition zones.  
766 The dotted black line corresponds with the southern limit of the ice sheet at LGM  
767 (extracted from Ehlers and Gibbard 2004). The blue line depicts the breakpoint where  
768 the temperature--*Carabus* richness relationship changes, as found in Calatayud et al.  
769 (2016b).

770

771 **Figure 3.** Results of the partial generalized matrix regression of similarity in regional  
772 co-occurrence, as a function of environmental niche similarity (climate and habitat),  
773 topographical connectivity and phylogenetic distances. The first and second bars  
774 correspond with the models including all regions and subregions, respectively. The  
775 remaining bars correspond with the models where the similarities in subregional  
776 occurrence were analysed independently for the species of each region. Con.= spatial  
777 connectivity; Envir. = environmental niche similarities; Overl.= Overlap.

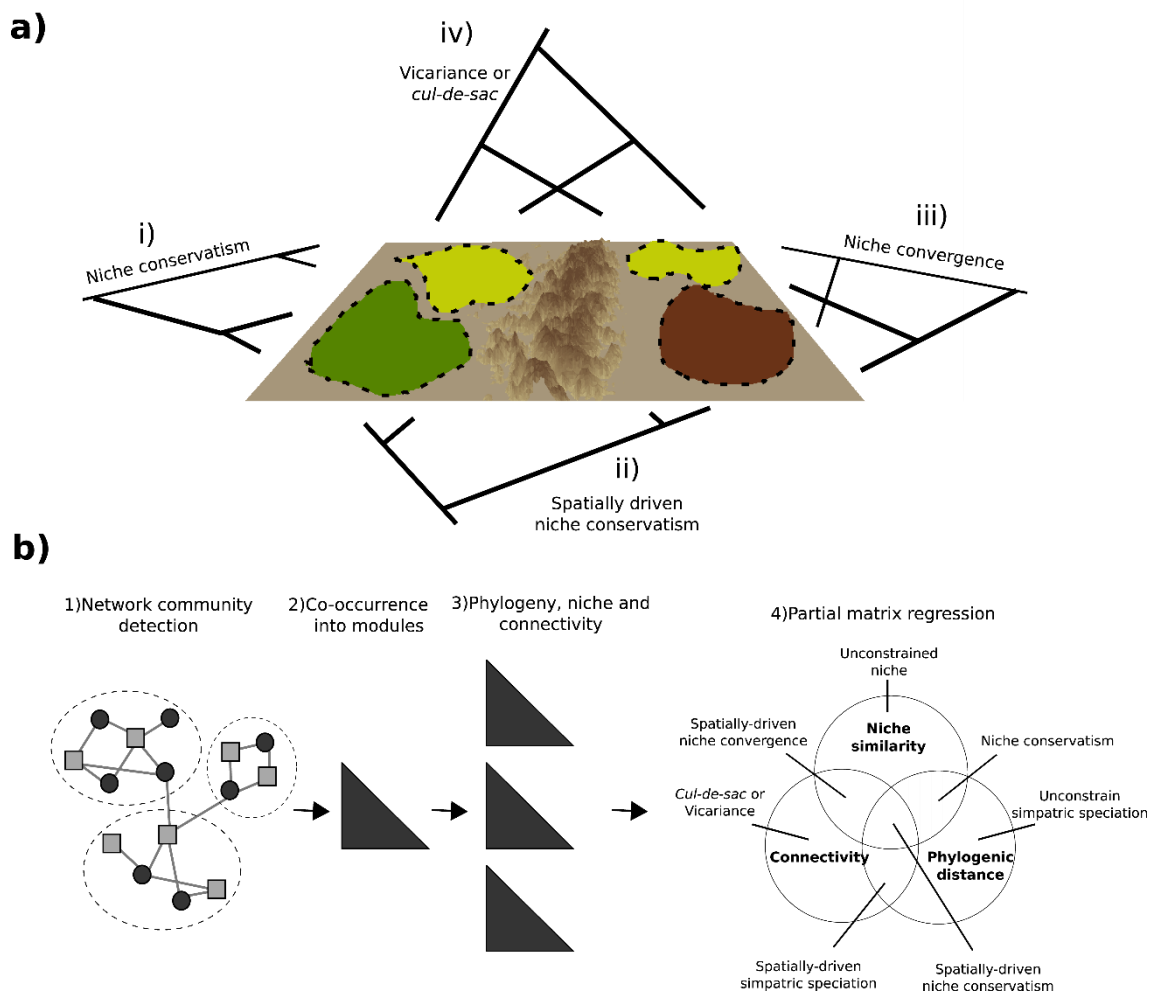
778

779 **Figure 4.** Results of the ancestral range estimation. a) Marginal probability of the most  
780 probable state at each internal node for a phylogenetic hypothesis where the  
781 BAREALIKE+J model was the best supported by the data. The size of the circles depicts  
782 the value of probability, while the colours represent the combinations of regions  
783 forming the state. The phylogeny is labelled at subgenera level. b) GAMM predictions  
784 of the marginal probability as a function of node age for the BAREALIKE+J model. The  
785 shaded area corresponds with the interval confidence at 95%. The dotted black line  
786 represent the breakpoint found by piecewise GLMM regression. The interval confidence  
787 at 95% for the breakpoint is also provided. See Fig. S5 for the predictions of the other  
788 models.  
789

790 **Figure 1.**

791

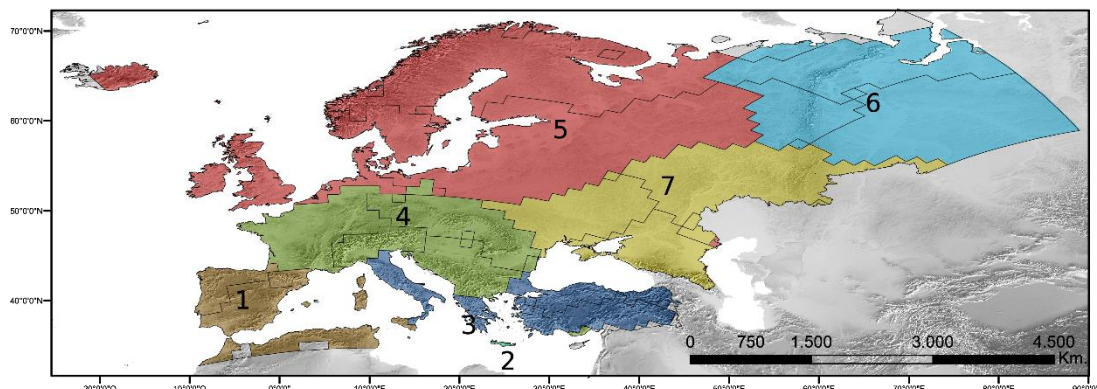
792



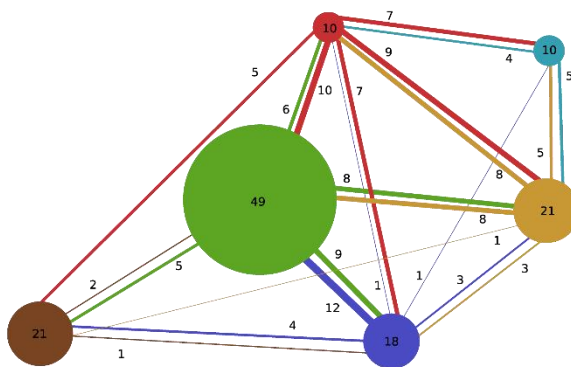
793

794 **Figure 2.**

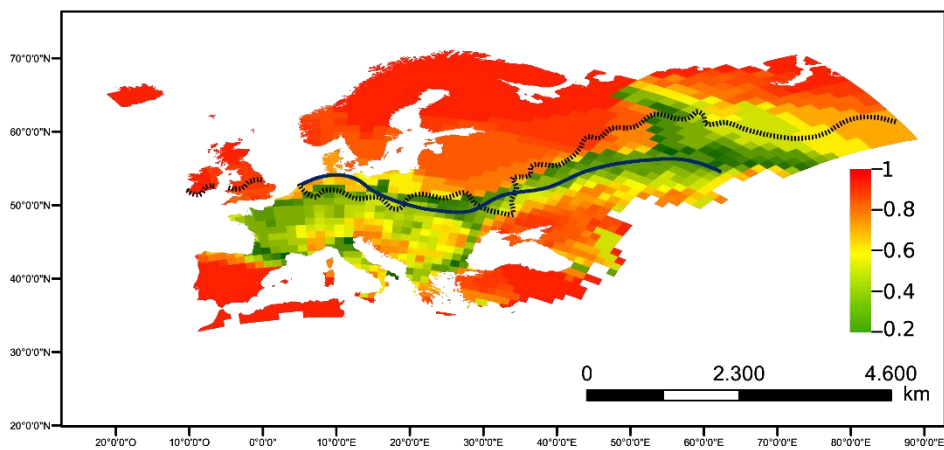
a)



b)



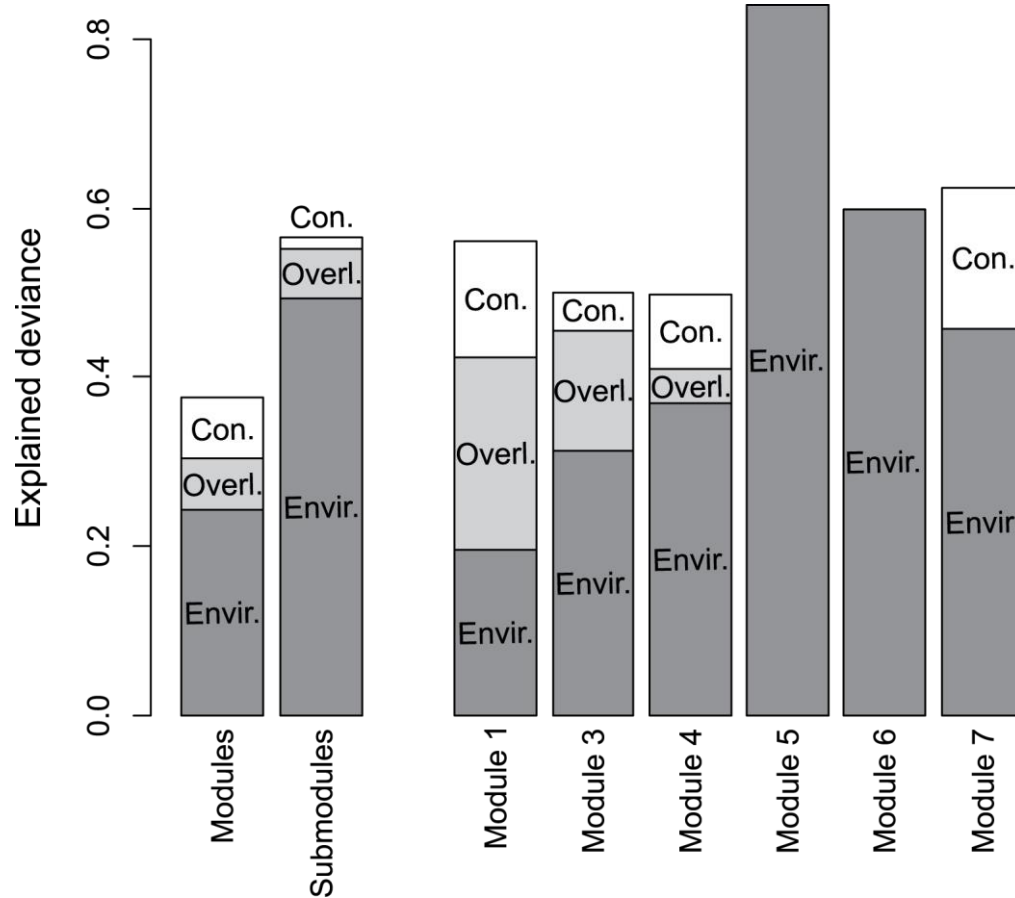
c)



795

796

797 **Figure 3**

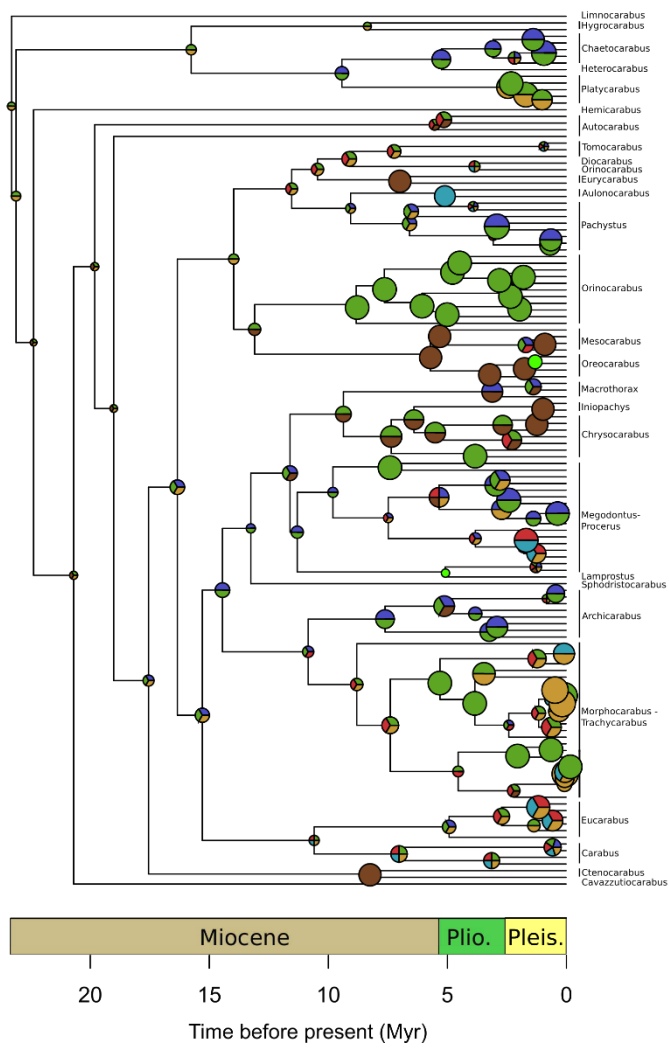


798

799

800 **Figure 4.**

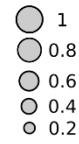
a)



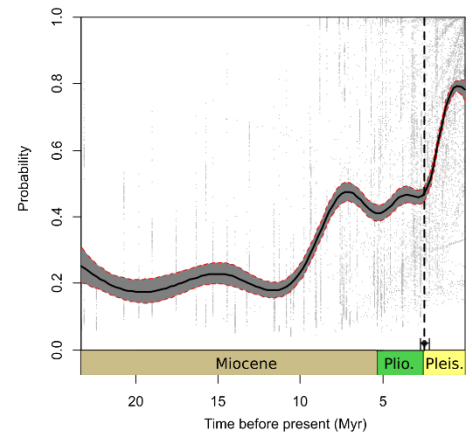
Color Legend



State probability



b)



801